Journal of Applied Mechanics and Technical Physics, Vol. 43, No. 6, pp. 830–835, 2002

SUPERCRITICAL FLOW OVER A SILL IN AN OPEN CHANNEL

V. I. Bukreev

UDC 532.59

Experimental data on typical profiles of free surface and channel bottom pressure for a supercritical flow over a sill are reported. This flow is shown to have, along with the known critical depth, two other characteristic depths, one of which is at the channel exit to the atmosphere and the other determines conditions under which the disturbances propagate well upstream of the sill. The experimental data are compared with calculation results based on a mathematical model that incorporates turbulent mixing upon wave breaking.

Introduction. In the theory of fluid wave motions, mathematical models have been lately developed that incorporate factors such as nonhydrostatic pressure distribution, nonuniform vertical distribution of velocity, presence of strong vorticity, mixing after wave breaking and loss of energy. These models are reviewed in [1]. On their basis, it is possible to calculate very complicated flows in more detail than on the basis of traditional models and to analyze important applied problems. In particular, calculations of unsteady motions in open channels are made, as a rule, on the basis of the Saint Venant equations [2–4]. These equations employ the hydrostatic law of pressure distribution over the flow depth. Although the Saint Venant equations incorporate energy losses (on the empirical basis), they are, in essence, the equations of the first approximation of shallow water theory and they do not describe, for example, waves of the undular bore type formed during the evolution of rather intense initial disturbances [5–7]. A bore with a breaking leading front is simulated in this model by a free surface discontinuity. The models taking into account the nonhydrostaticity of pressure distribution and mixing simulates the real processes more adequately [8].

Testing and further development of new models require additional experimental information for a number of classical problems of hydraulics in that range of determining parameters in which the previously used models diverge substantially from the experiment. One of such problems — the flow over a sill on the bottom of an open channel — is considered in the present work. This flow has 10 strongly differing regimes. This paper gives examples of the most typical flow regimes for the case where the incident flow is supercritical.

The most detailed investigation of sill overflow was made primarily to determine the discharge coefficient in the subcritical regime (see, for example, [9, 10]). Smyslov [11] proposed one of the first theories that incorporated the nonhydrostaticity of pressure distribution in subcritical sill overflow. The greatest number of experimental data for the case of supercritical incident flow was obtained primarily in studies of the motion of a streamlined obstacle in a steady, density stratified fluid flow [12, 13]. Under certain assumptions, these data can be extended to the case of sill overflow in a homogeneous fluid, using the principle of motion reversal and considering free-surface flow as a special case of a two-layer fluid [12]. One should take into account that both assumptions have a limited field of application [14].

Experimental Procedure. The experiments were performed in a rectangular channel of Plexiglas, 390 cm long and $B = 6$ cm wide, with zero bottom slop. Supercritical (rapid) flow was generated by a nozzle, whose internal surface was profiled by a hyperbolic tangent. Measurements showed that at the nozzle outlet there were a local depression of the free surface level (by about 4% of the nozzle outlet height) and a local decrease in channel bottom pressure (by about 6% of the hydrostatic pressure). The sill was placed outside the influence of these local nonuniformities, which were manifested at a downstream distance not exceeding the nozzle height.

Lavrent'ev Institute of Hydrodynamics, Siberian Division, Russian Academy of Sciences, Novosibirsk 630090.
Translated from Prikladnaya Mekhanika i Tekhnicheskaya Fizika, Vol. 43, No. 6, pp. 54–61, November–December, 2002. Original article submitted May 14, 2002.

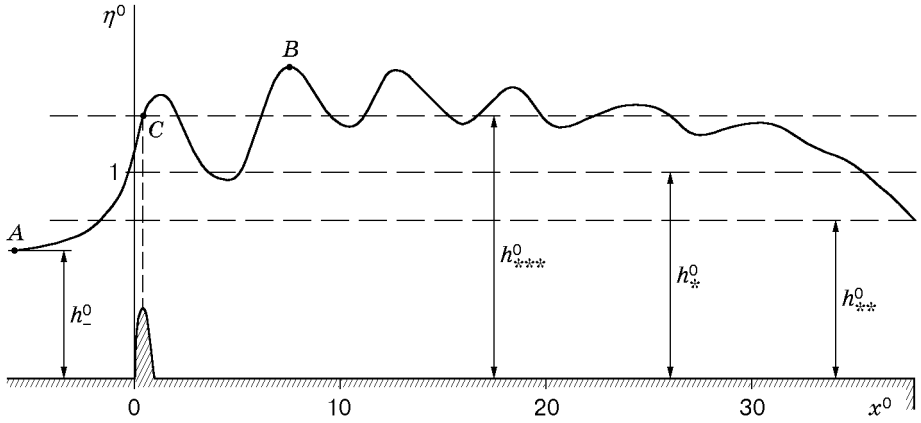

Fig. 1. Free-surface profile behind sill 1 ($h_* = 4$ cm, $b^0 = 0.35$, and Fr = 2.63).

It should be noted that for a channel of limited length, the method of level regulation in its outlet section is of great importance. For example, if the flow is compressed from the top by a vertical plate, the incident waves can be reflected from it. If a regulating plate compresses the flow from the bottom and the flow behind it enters the atmosphere, then no wave reflection is observed. However, in this case, at an upstream distance, the mean position of the free surface level changes, which leads to wave transformation due to a change in flow depth. In this study, both methods of regulation were used.

The experiments were performed with sills of various shapes and dimensions made of Plexiglas. The sill 1 had the shape of a circular segment. Its radius R and height b (and, therefore, length l) were varied. The sill 2 had a rectangular cross section of height b and length l. We also considered the case of a step where the back face of the rectangular sill was in the channel outlet section (sill 2a). The sill 3 had a streamlined shape. Its front face was delineated by a circular arc with a radius of 14 cm, the upper face was a horizontal plane and the back face was a plane inclined to the channel bottom at an angle of 11°. The height of this sill $b = 2.4$ cm and its length $l = 30$ cm were not varied. The sill 3a differed from the sill 3 only in the shape of the front face. This face was delineated by a hyperbolic tangent equation instead of a circle equation, since in supercritical flow the use of a sharpened leading front is preferred to a rounded one. The upper and back faces were not varied. The total length of the sill increased to 50 cm. The experiments showed that, everything else equal, the difference in the free-surface profiles over the sills 3 and 3a did not exceed the measurement error.

The volumetric discharge of the fluid Q was measured by a standard Venturi tube located in the supplying pipeline. The flow depth at different points along the channel length was determined with measuring needles. The mean velocity was measured with a Pitot tube and piezometers. The standard measurement error did not exceed 0.5% for discharge, 1% for velocity, and 1% for depth. For visualization of the flow structure, particles of aluminum powder were introduced into the flow. Photo and video recording were also employed.

Results of the experiments show that for steady nonuniform flow in an open channel, in particular, in transition from one flow regime to another, the following three characteristic depths play an important role:

$$h_* = \sqrt[3]{q^2/g}, \quad h_{**} \approx 0.77 h_*, \quad h_{***} \approx 1.27 h_*.$$

Here $q = Q/B$ is the discharge intensity (per unit of channel width) and g is the acceleration of gravity. The values of the coefficients are obtained by experiment. In hydraulics, h_* is called a critical depth [9, 10]. A flow of depth $h > h_*$ is called subcritical (calm), and a flow of depth $h < h_*$ is called supercritical (rapid) [9, 10]. In the range of values $h \approx h_{**}$, the shape of the hydraulic jump changes. For an incident flow of depth $h_- < h_{**}$, a classical hydraulic jump with a roller in its head takes place, and in the range $h_{**} < h_- < h_*$, a smooth undular jump forms. Below we consider examples in which the value of the characteristic depth h_{**} is important along with h_*. The depth h_{***} is conjugate with h_{**} (the meaning of this term is explained in [9, 10]). In plotting, the linear dimensions were normalized to h_*. Dimensionless quantities are denoted by the superscript 0. The characteristic Froude number is defined as

$$\mathrm{Fr} = q/(h_- \sqrt{g h_-}\,) = (h_*/h_-)^{3/2}.$$

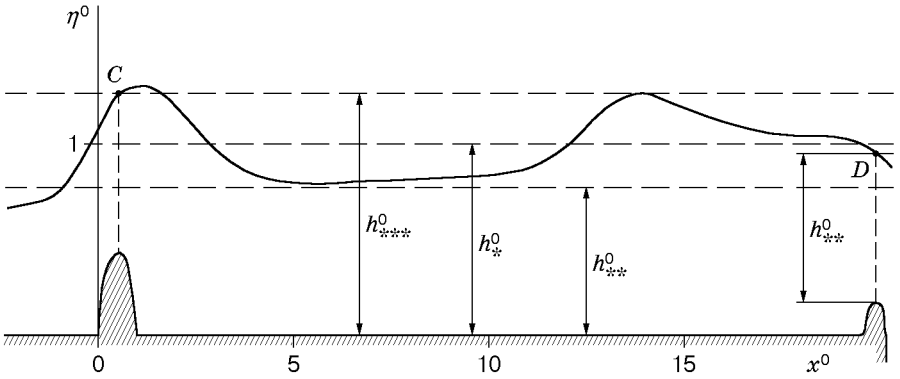

Fig. 2. Free-surface profile between two sills 1 ($h_* = 7.65$ cm, Fr = 3.7, $b^0 = 0.431$, and $b_1^0 = 0.183$).

Experimental Results. Figure 1 shows free-surface profile $\eta^0(x^0)$ (x^0 is the dimensionless longitudinal coordinate) in the neighborhood of the sill 1 for the case where the exit flow freely enters the atmosphere and the depth of the incident flow $h_- < h_{**} < h_*$. In the absence of the sill, the flow remained supercritical up to the exit from the channel. In the presence of the sill, intense nonlinear waves formed, which actually are a variety of a smooth undular hydraulic jump but have some special features.

The points A and B in Fig. 1 correspond to reciprocally conjugate values of η^0 calculated from the following formula [9, 10]:

$$\eta_B^0 = \eta_A^0[\sqrt{1 + 8/(\eta_A^0)^3} - 1]/2. \tag{1}$$

Over the flat bottom, the ratio of the conjugate depths for which the free-surface profile in Fig. 1 was obtained corresponds to the region of existence of perfect hydraulic jumps with a roller at its head [9]. However, in the experiment, a smooth undular jump occurred. Thus, this example shows that in the presence of a sill, the region of existence of smooth undular jumps increases.

An interesting feature of the example considered is that at the exit channel, the characteristic depth h_{**}^0 is established, and immediately over the sill crest (at the point C), $\eta_C^0 = h_{***}^0$. As a result, undulations occur mainly in the subcritical flow in the neighborhood of the depth h_{***}^0 rather than the depth η_B^0, as would be the case for an undular jump over a flat bottom. Therefore, other things being equal, the potential energy of a flow with an undular jump is lower behind a sill than over a flat bottom.

In this case, perturbations do not propagate well upstream. The experiments show (see below) that in the case of a streamlined sill, for perturbations to propagate well upstream, the free-surface level over the crest (at the point C) must exceed the characteristic conjugate depth h_{***}^0. In the example considered, the state of the flow is nearly critical. With a 3% decrease in discharge, a bore with a breaking leading front was propagating upstream of the sill.

Figure 2 shows a free-surface profile behind the same sill as in Fig. 1 but with a larger value of Fr. In addition, at the channel exit there is an obstacle in the form of a sill of the same type but of lower height: $b_1^0 = 0.183$. A solitary hump ("soliton") and a stretched valley with supercritical flow are formed behind the main sill of height $b^0 = 0.431$. Another "soliton" in Fig. 2 is formed under the influence of the specific conditions at the channel exit. Other conditions can lead to the formation of an undular or a classical hydraulic jump. We note that in the example considered, the characteristic depth h_{**}^0 is also formed at the channel exit, i.e., at the point D in Fig. 2 the relation $\eta_D^0 = h_{**}^0 + b_1^0$ holds. Thus, the range in which this regularity holds is extended to that obtained before, in particular, for subcritical flow.

In contrast to the example in Fig. 1, the state of this flow is far from critical, under which waves begin to propagate upstream of the obstacle. Nevertheless, directly over the sill crest, $\eta_C^0 \simeq h_{***}^0$. Therefore, this condition (convenient in mathematical modeling) holds within a sufficiently wide range of parameters, whose boundaries are to be studied. We can note tentatively that the sill must be streamlined and sufficiently short so that the maximum of the "soliton" formed over it is displaced downstream of the sill crest.

Figure 3 shows flow over the sill 2a (step) for the case where a classical hydraulic jump is formed behind the sill. Of special interest are two facts. First, before the jump (at the C point), the relation $\eta_C^0 = h_{**}^0$ holds. Second, the free-surface levels at the points A and B are mutually conjugated by (1) obtained for the jump over the flat

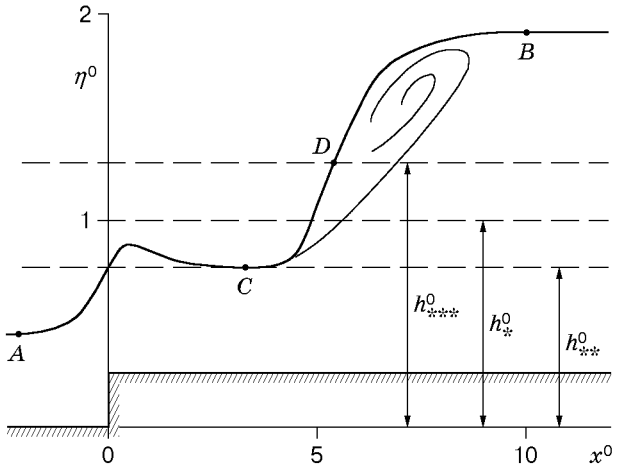

Fig. 3. Classical hydraulic jump behind a step (sill 2a) ($h_* = 4.2$ cm, $b^0 = 0.26$, and Fr = 3.11; distance from the step to the channel exit $l^0 = 21$).

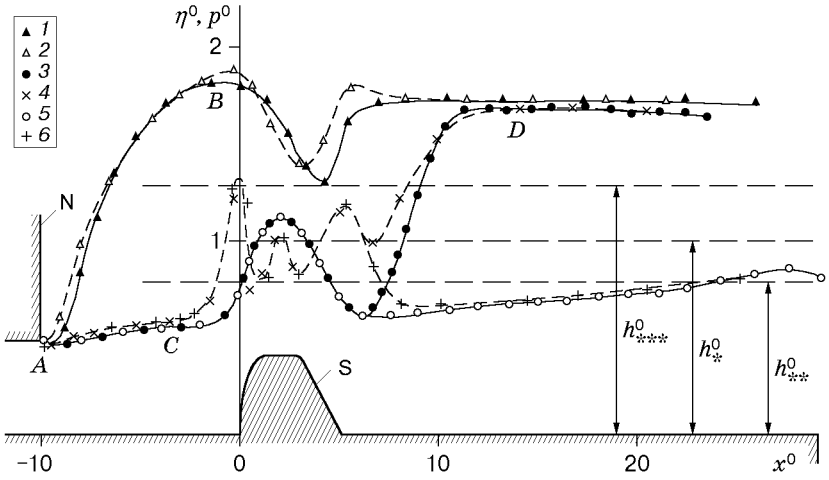

Fig. 4. Profiles of free-surface η^0 (1, 3, and 5) and channel bottom pressure p^0 (2, 4, and 6) at $h_* = 5.8$ cm, $b^0 = 0.42$, Fr = 2.75, and $h^0_+ = 1.7$ (1 and 2), 1.6 (3 and 4), and $h^0_+ = h^0_{**}$ (6 and 7); N denotes the nozzle and S denotes the sill 3.

bottom. Therefore, there exists a range of flow parameters in which the classical equation (1) is also applicable to hydraulic jumps in a channel with a step.

It should also be noted that in the example considered, the perturbation does not propagate well upstream, although on the free-surface profile there is a point D at which $\eta^0_D = h^0_{***}$. This point is away from the step and is preceded by supercritical flow. The perturbation began to propagate upstream under a combination of parameters such that the point D was directly above the step.

Figure 4 shows results of experiments with the sill 3. The channel bottom pressure distribution $p^0(x^0)$ is shown along with curves of $\eta^0(x^0)$. The pressure is normalized to $\rho g \eta$ (ρ is the fluid density), so that according to the hydrostatic law of pressure distribution, the relationship $p^0 = \eta^0$ must hold. In this series of experiments, the tail-water depth h_+ was varied with unchanged values of h_* and h_-.

The points 5 and 6 were obtained for the case where the level regulator was absent from the channel outlet section and the flow was supercritical both ahead of the sill and at an appreciable distance behind it. According to the theory of ideal fluid, a bump is formed over the sill, and behind the sill, the free-surface level increases monotonically under the action of friction on the bottom and the walls of the channel. At the exit from the channel, as in the example in Figs. 1 and 2, the depth h^0_{**} was established. The pressure distribution differs from hydrostatic pressure only over the sill and at distances of $2h_*$ and $5h_*$ ahead of and behind the sill, respectively.

TABLE 1

Variant 1			Variant 2			Variant 3		
x^0	η^0	p^0	x^0	η^0	p^0	x^0	η^0	p^0
−10.9	—	0.61	−10.9	—	0.61	−11	- –	0.61
−10	0.50	0.46	−10	0.50	0.46	−10.2	0.51	0.50
−9.5	0.48	0.50	−8.5	0.49	0.50	−9.5	0.50	0.50
−7	0.52	0.54	−7	0.53	0.53	−9	0.51	0.66
−5	0.55	0.57	−5	0.55	0.57	−8	0.90	1.00
−3	0.56	0.60	−3	0.56	0.59	−7	1.22	1.24
−2	0.56	0.66	−2	0.57	0.65	−5	1.58	1.58
−1	0.59	0.85	−1	0.59	0.85	−3	1.75	1.75
−0.25	0.68	1.25	−0.25	0.68	1.30	−1.5	1.80	1.80
0.45	0.86	0.97	0.45	0.86	0.95	−0.3	1.80	1.90
1.4	1.05	0.81	1.40	1.07	0.82	0.5	1.78	1.79
2.1	1.08	1.04	2.1	1.09	1.05	1.45	1.68	1.59
3	1.06	0.83	3	1.06	0.84	2.2	1.55	1.55
4	0.89	0.89	4	0.89	0.89	3	1.40	1.39
5.3	0.66	1.17	5.3	0.66	1.17	4	1.30	1.50
7	0.62	0.81	6.2	0.60	1.00	5.4	1.61	1.76
8	0.62	0.67	7	0.66	1.02	7	1.68	1.68
9	0.63	0.66	8	0.81	1.20	9	1.68	1.68
12	0.65	0.67	9	1.22	1.35	12	1.68	1.68
14	0.67	0.69	10	1.50	1.50	15	1.68	1.68
20	0.71	0.73	11.5	1.65	1.65	20	1.69	1.68
24	0.75	0.76	15	1.65	1.65	25	1.69	1.69
26	0.81	0.81	17.5	1.66	1.66	—	—	—

Notes. Variant 1 corresponds to the following experimental conditions: $h_* = 5.8$ cm, $h_-^0 = 0.5$, and $h_+^0 < h_*$ (no jump), variant 2 to $h_* = 5.8$ cm, $h_-^0 = 0.5$, and $h_+^0 = 1.65 > h_*$ (jump behind the sill), and variant 3 to $h_* = 5.7$ cm, $h_-^0 = 0.51$, and $h_+^0 = 1.68 > h_*$ (jumps before and behind the sill).

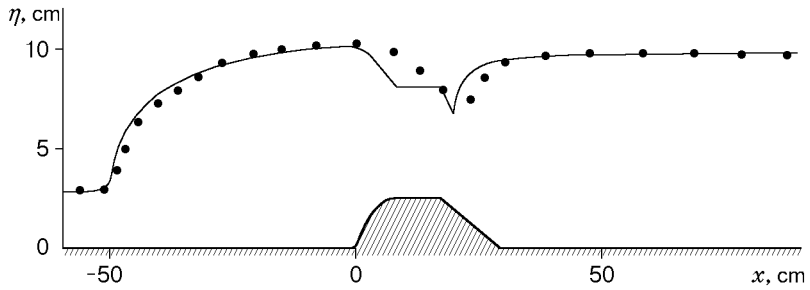

Fig. 5. Comparison of experimental and calculated data for the sill 3 ($h_* = 5.8$ cm, $b^0 = 0.42$, Fr = 2.75, and $h_+^0 = 1.7$).

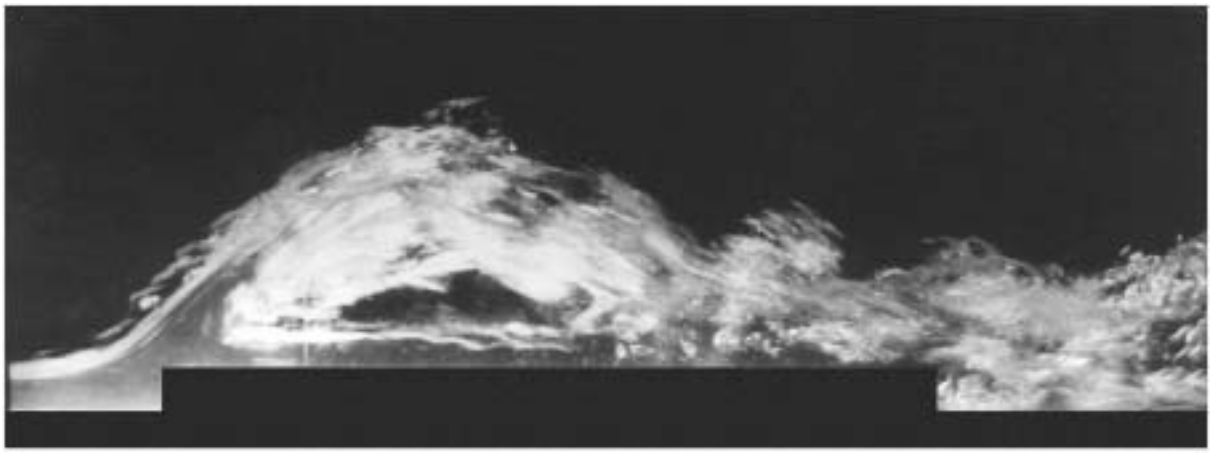

Fig. 6. Air cavity above the sill 2 ($h_* = 4.1$ cm, $b^0 = 0.34$, $l^0 = 5.62$, and Fr = 3.91).

The points 3 and 4 were obtained under a substantial increase of the depth h_+ compared to the previous example using a vertical plate protruding over the bottom at the channel exit. Behind the sill, a classical hydraulic jump formed, and the flow over and ahead of the sill remained the same as in the previous example. In hydraulics, such a regime of sill overflow is called nonsubmerged flow [9, 10]. The depths at the points C and D are mutually conjugated by (1). This example confirms the existence of a parameter range in which the presence of a sill does not affect the values of the conjugate depths obtained for a flat bottom.

The points 1 and 2 are obtained for the case where the depth h_+ is increased by only 6.3% compared to the case corresponding to the points 3 and 4. However, this has led to the formation of two hydraulic jumps with a roller at the head: ahead of and behind the sill. For the jump ahead of the sill, the conjugate depths are established at the points A and B, and for the jump behind the sill, the points C and D still correspond to the conjugate depths. In this example, the departure from the hydrostatic law is negligible and occurs only over the back face of the sill.

Conclusions. Current mathematical models describe the flow under consideration over a rather wide range of parameters. Figure 5 shows results of verification of the mathematical model of [1, 8], which incorporates the turbulent mixing process upon wave breaking. The experimental points correspond to the points 1 in Fig. 4, and the solid curve refer to calculation results. The model satisfactorily describes even a complicated flow regime with two hydraulic jumps. For testing other models, the obtained experimental data are tabulated.

At the same time, sill overflow involves complicated processes, whose mathematical modeling requires novel approaches. As an example, Fig. 6 shows a photograph of a cavity resulting from flow separation from the leading front of the sill. The strong fluid discontinuity observed in Fig. 6 occurs for rather large values of Fr and b^0. Cavities are also formed behind the sill [15]. In contrast to them, the cavity in Fig. 6 has no contact with any of the solid boundaries.

The author thanks A. V. Gusev for assistance in the experiments and in preparation of this paper.

This work was supported by the Russian Foundation for Fundamental Research (Grant No. 01-01-00846) within the framework of the Program of Support of Leading Scientific Schools of Russia (Grant No. 00-05- 98542) and Integration Project No. 1 SD RAS.

REFERENCES

1. V. Yu. Liapidevskii and V. M. Teshukov, "Mathematical models of propagation of long waves in an inhomogeneous fluid," *Izd. Sib. Otd. Ross. Akad. Nauk*, Novosibirsk, (2000).
2. R. E. Dreisler, "Comparison of Theories and Experiments for the Hydraulic Dam-Break Wave," *Int. Assoc. Sci. Hydrology*, No. 38, 319–328 (1954).
3. J. J. Stoker, *Water Waves. Mathematical Theory and Applications*, Interscience Publishers, New York (1957).
4. M. T. Gladyshev, "On propagation of discontinuities in open channels" *Izv. Vyssh. Uchebn. Zaved., Energ.*," No. 11, 70–77 (1965).
5. H. Favre, *Ondes de Translation Dans Les Canaux Decoverts*, Paris, Dunod (1935).
6. V. I. Bukreev and A. V. Gusev, "Waves before a vertical plate in a channel," *Izv. Ross. Akad. Nauk, Mekh. Zhidk. Gaza*, No. 1, 82–90 (1999).
7. V. I. Bukreev and A. V. Gusev, "Waves ahead of an underwater wing. Experiment," *Izv. Ross. Akad. Nauk, Mekh. Zhidk. Gaza*, No. 4, 72–80 (2001).
8. V. I. Bukreev, A. V. Gusev, and V. Yu. Liapidevskii, "Blocking effects in supercritical flows over topography," in: *PIV and Modeling Water Wave Phenomena*, Proc. of the Int. Symp. (Cambridge, UK, April 17–19, 2002), Univ. of Oslo (2002), pp. 86–90.
9. P. G. Kiselyev, *Handbook on Hydraulic Calculations* [in Russian], Gosénergoizdat, Moscow–Leningrad (1957).
10. Ven Te Chow, *Open-Channel Hydraulics*, McGraw Hill, New York (1959).
11. V. V. Smyslov, *Theory of Spillway with a Wide Sill* [in Russian], Izd. Akad. Nauk UkrSSR, Kiev (1956).
12. P. G. Baines, *Topographic Effects in Stratified Flow*, Cambridge Univ. Press, Cambridge (1995).
13. V. I. Bukreev and N. V. Gavrilov, "Perturbations ahead of a wing moving in a stratified fluid," *J. Appl. Mech. Tech. Phys.*, No. 2, 257–259 (1990).
14. V. I. Bukreev, "Undular jump in open sill overflow in the channel," *J. Appl. Mech. Tech. Phys.*, **42**, No. 4, 596–602 (2001).
15. V. I. Bukreev and A. V. Gusev, "Cavities behind the spillway with a wide sill," *J. Appl. Mech. Tech. Phys.*, **43**, No. 2, 280-285 (2002).